Kinetic Study of Phosphorylation-Dependent Complex Formation between the Kinase-Inducible Domain (KID) of CREB and the KIX Domain of CBP on a Quartz Crystal Microbalance

Hisao Matsuno, Hiroyuki Furusawa, and Yoshio Okahata*[a]

Abstract: We report quantitative analysis of peptide–peptide interactions on a 27 MHz quartz crystal microbalance (QCM) in aqueous solution. The KID (kinase-inducible domain) of transcription factor CREB (cyclic AMP response element binding protein) is known to interact with the KIX domain of coactivator CBP (CREB binding protein), facilitated by phosphorylation at Ser-133 of the KID. The KIX domain peptide (86 aa) was immobilized on the QCM gold electrode surface by means of a poly(ethylene glycol) spacer. Binding of the KID peptide (46 aa) to the KIX peptide was detected by frequency decreases (mass increases) of the QCM. Both maximum binding amount (Δm_{max}) and association constants (K_a) obtained from the QCM measurements increased as a result of phosphorylation of Ser-133 of the KID peptide. The K_a values for KIX peptide to the phosphorylated (pKID) and unphosphorylated KID peptides were $(93\pm2)\times10^3$ and $(5\pm1)\times10^3\,\text{M}^{-1}$, respectively. This difference was explained by the dissociation rate constant (k_{-1}) of the pKID being 20 times smaller than that of the KID, while association rate constants (k_1) were independent of phosphorylation.

Keywords: kinetics · peptide–peptide interactions · phosphorylation · protein kinases · quartz crystal microbalance

Introduction

Phosphorylation-dependent protein–protein interactions provide the foundation for a multitude of intracellular signal transduction pathways, and a number of signaling pathways have been shown to regulate the expression of target genes by the phosphorylation of specific transcription factors.[1] In the most common mechanism of activation of transcription processes, basal transcription factors are recruited by activators through either direct interactions with components of the transcriptional factors or indirect interactions mediated by coactivators.[2] A subset of these activator and coactivator associations is subject to further regulation by reversible covalent modifications, such as protein phosphorylation.[1,3]

One of the best characterized stimulus-induced transcription factors, cyclic AMP (cAMP) response element binding protein (CREB), plays a role in mediating the transcriptional response invoked by intracellular second messenger cAMP in response to extracellular stimuli.[4,5] Activation of the kinase-inducible domain (KID) is dependent on phosphorylation of a particular residue, Ser-133, by a protein kinase A (PKA).[6] Phosphorylation of Ser-133 in turn induces interaction with the KIX domain of the CREB binding protein (CBP).[7–10] NMR studies revealed a direct role for the phosphate group of phosphoserine-133 (pSer-133) in the formation of the complex pKID–KIX. The phosphate group engages in intermolecular interactions with the hydroxyl group of Tyr-658 and the ε-amino group of Lys-662 of the KIX domain.[11] Recently, an *E. coli* based two-hybrid system was applied to examine this phosphorylation-dependent KID–KIX interaction, providing a rapid and simple selection system for detecting protein–protein interactions in *E. coli*.[12]

The nature of biomolecular interactions, such as DNA–protein, RNA–protein, and protein–protein, can be understood more precisely by using kinetic analyses to complement structural NMR spectroscopic and X-ray crystallographic studies. We have reported quantitative kinetic studies of biomolecular interactions, such as DNA hybridization,[13] the binding of transcriptional regulation factor GCN4-bZIP peptide to its target DNA,[14] the binding of replication factor PCNA to DNA,[15] and enzymatic reactions, such as polymerase on DNA,[16–18] by using a DNA-immobilized 27 MHz quartz crystal microbalance (QCM). A QCM is a very sensitive device for mass measurement, in both air and aqueous solution. Its oscillatory resonance fre-

[a] Prof. H. Matsuno, Prof. H. Furusawa, Prof. Y. Okahata
Department of Biomolecular Engineering
Tokyo Institute of Technology and CREST, JST
4259 Nagatsuda, Midori-ku, Yokohama 226–8501 (Japan)
Fax: (+81) 45-924-5781
E-mail: yokahata@bio.titech.ac.jp

Supporting information for this article is available on the WWW under http://www.chemeurj.org/ or from the author.

DOI: 10.1002/chem.200400030

quency decreases linearly as the mass on the QCM electrode increases (at the nanogram level).[19,20] The 27 MHz QCM used in this study has an ideal sensitivity of 0.62 ng cm^{-2} change in mass per one Hz reduction in frequency, a sensitivity sufficient to detect peptide–peptide interactions.[21]

As described above, protein phosphorylation is one of the key mechanisms of specific protein–protein interaction; however, little is known of the kinetics of this process. In this paper, we apply a QCM method to provide kinetic analysis of phosphorylation-dependent peptide–peptide interactions (Figure 1). The KIX domain peptide (86 aa; aa = amino acid) of coactivator CBP was immobilized on the QCM plate, and the binding of the KID of CREB was monitored by measuring frequency decreases (mass increases). The maximum binding amounts (Δm_{max}), association constants (K_a), and association and dissociation rate constants (k_1 and k_{-1}) were obtained and subsequently compared following phosphorylation of KID and variation of ionic strength.

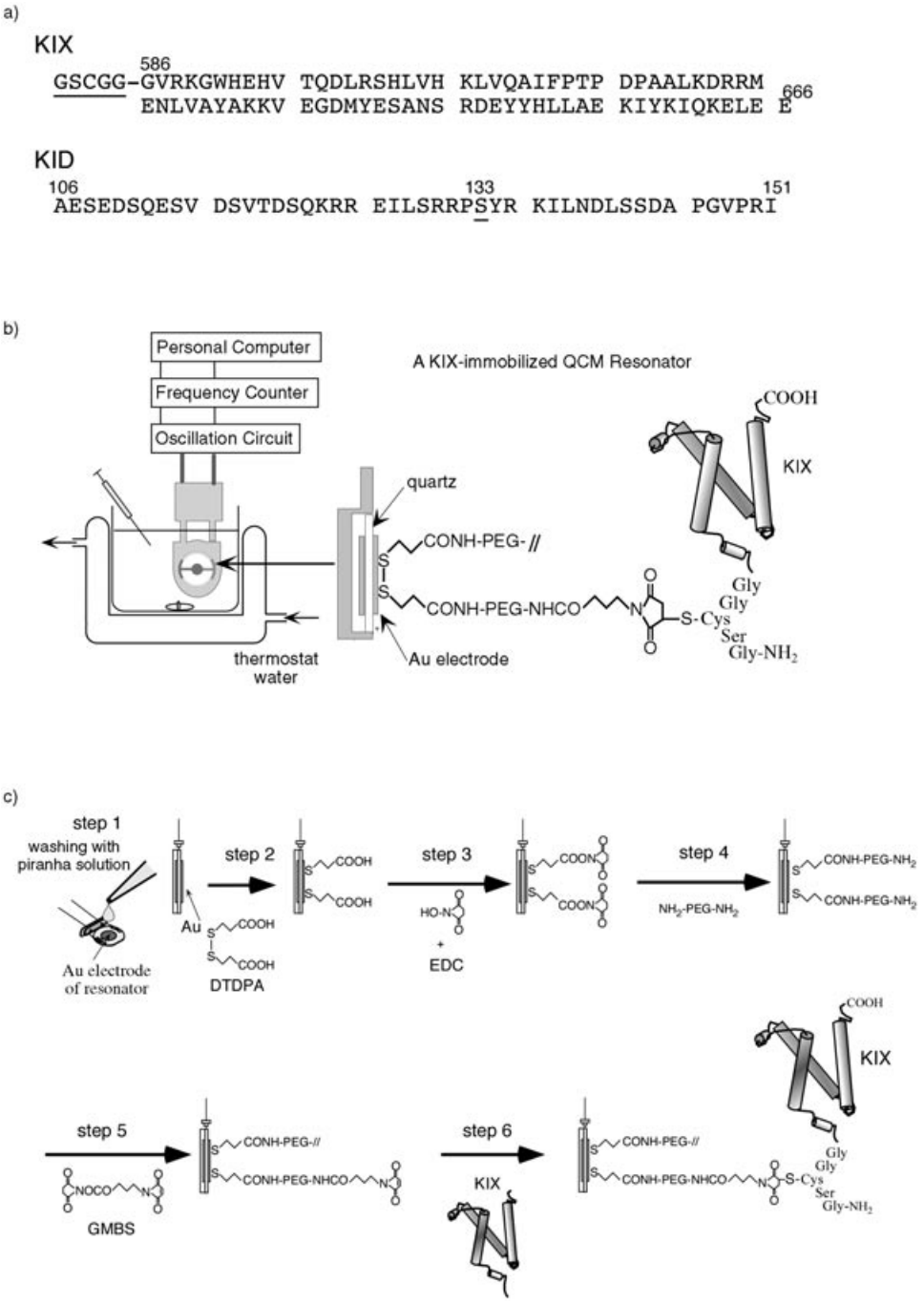

Figure 1. a) Peptide sequences of the KIX domain of mCBP (residues 586–666) and the KID of mCREBα (residues 106–151). A GSCGG linker (underlined) attached to the N terminus of KIX enabled immobilization to the Au electrode of a QCM plate by binding of the -SH group of the Cys residue. Phosphorylation at Ser-133 of the KID mediates interaction with the KIX domain. b) A representation of a 27 MHz QCM for monitoring the binding of the KID or the pKID to the KIX-immobilized QCM resonator. c) Immobilization of the KIX peptide to the Au electrode of a QCM resonator (see Experimental Section for details).

Results and Discussion

Saturation binding of pKID or KID to KIX on the QCM: Figure 2a shows the typical frequency changes for the KIX domain-immobilized QCM resonator, responding to additions of pKID or KID peptides in solution. Mass increases due to binding of pKID to KIX were observed; however, nonphosphorylated KID binding was barely detectable under the same conditions. Binding amounts (Δm) revealed simple saturation curves as a function of peptide concentrations, as shown in Figure 2b. In control experiments, very low levels of binding of both the pKID and KID peptides to the PEG-immobilized QCM under the same conditions were detected. In addition, binding of the pKID or KID peptides to the KIX-immobilized QCM was inhibited by free KIX peptides in the solution in a concentration-dependent manner. These results clearly indicate the specific peptide–peptide interaction between KIX and pKID or KID.

The saturation binding kinetics of Figure 2b are expressed by Equation (1) as linear reciprocal plots of [peptide]/Δm against [peptide], as shown in Figure 2c.[22]

$$\frac{[KID]_0}{\Delta m} = \frac{[KID]_0}{\Delta m_{max}} + \frac{1}{K_a \Delta m_{max}} \quad (1)$$

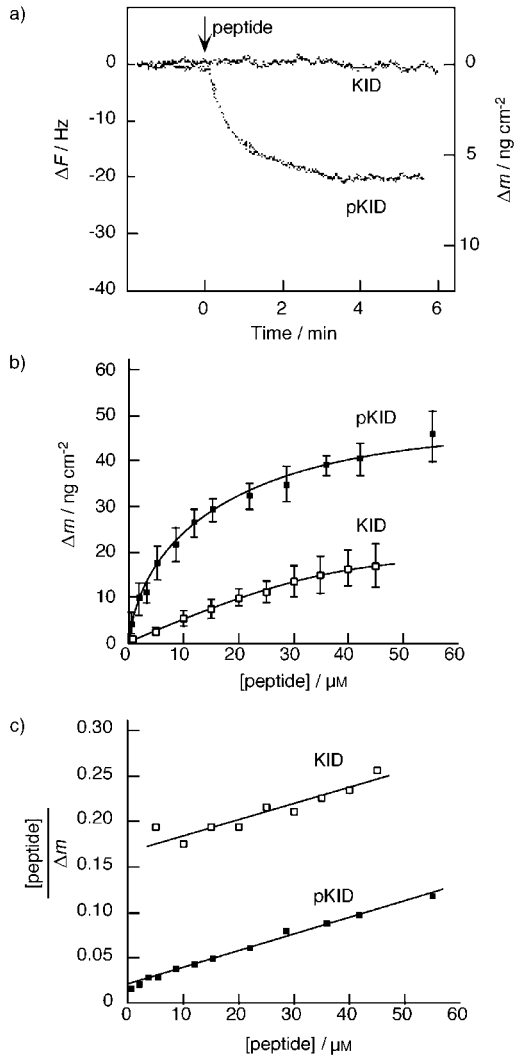

Figure 2. a) Typical time courses of the frequency change of the KIX-immobilized QCM resonator, responding to the addition of the KID or pKID peptides. [pKID] = [KID] = 2 μM in 10 mM HEPES, pH 7.9, 100 mM KCl, 5 mM $MgCl_2$, 0.1 mM EDTA, 0.1 % Nonidet P-40, 20 °C. b) Saturation binding behaviors of pKID and KID peptides to the KIX as a function of added peptide concentrations (10 mM HEPES, pH 7.9, 100 mM KCl, 5 mM $MgCl_2$, 0.1 mM EDTA, 0.1 % Nonidet P-40, 20 °C). c) Linear reciprocal plots of Figure 2b.

Association constants (K_a) and maximum binding amounts (Δm_{max}) were calculated from the slope and intercept, respectively, of Figure 2c. We found that pKID bound to KIX with a K_a of $(93 \pm 9) \times 10^3\,M^{-1}$ and a Δm_{max} of $51 \pm 2\,ng\,cm^{-2}$ ($9.7\,pmol\,cm^{-2}$). The binding characteristics of nonphosphorylated KID ($K_a = (5 \pm 1) \times 10^3\,M^{-1}$, $\Delta m_{max} = 20 \pm 5\,ng\,cm^{-2}$) were significantly decreased compared with those of pKID. The results obtained are summarized in Table 1.

The ideal maximum binding expected for the binding of one pKID molecule to one KIX molecule on the QCM surface is calculated to be $64\,ng\,cm^{-2}$; therefore, a Δm_{max} of $51 \pm 2\,ng\,cm^{-2}$ indicates that approximately 80 % of the KIX molecules on the electrode surface bind pKID molecules. This also suggests that nonspecific peptide adsorption may be insignificant under these conditions. Some binding of the nonphosphorylated KID peptide was also observed under the same conditions; however this is not a nonspecific interaction with the QCM surface, as it is inhibited by the addition of free KIX peptide.

Table 1. Kinetic parameters for binding of pKID and KID to KIX on the QCM.[a]

peptide	Saturation binding[b]		Curve fitting[c]		
	Δm_{max} [ng cm^{-2}]	K_a [10^3 M^{-1}]	k_1 [M^{-1}s^{-1}]	k_{-1} [10^{-3}s^{-1}]	K_a [10^3 M^{-1}]
pKID	51 ± 2	93 ± 9	130 ± 20	1.4 ± 0.2	93 ± 2
KID	20 ± 5	5 ± 1	120 ± 20	25 ± 1	5 ± 1

[a] 10 mM HEPES, pH 7.9, 100 mM KCl, 5 mM $MgCl_2$, 0.1 mM EDTA, 0.1 % Nonidet P-40, 20 °C. [b] Obtained from Equation (1). [c] Obtained from Equation (5) and $K_a = k_1/k_{-1}$.

Effect of ionic strength: In general, electrostatic forces strongly govern intermolecular interactions between peptides. In order to reveal electrostatic contributions to the KID–KIX interaction, salt concentrations in the range of [KCl] = 10–800 mM were used, and Δm_{max} and K_a values were obtained at each ionic concentration (Figure 3). Over the range of 10–400 mM of KCl, the Δm_{max} values of pKID were independent of ionic strength; however, they decreased remarkably at 800 mM KCl. On the other hand, the Δm_{max} values for the nonphoshorylated KID peptide decreased at comparatively lower ionic strength. Although the pKID showed the greatest binding to the KIX in the presence of 200 mM KCl, KID binding simply decreased as ionic strength increased.

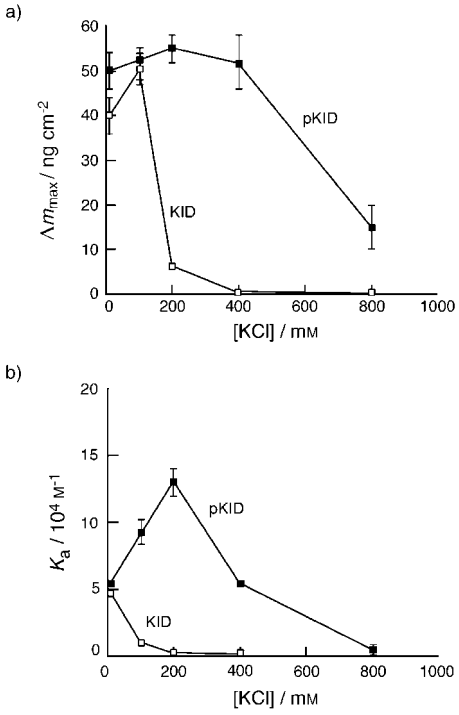

Figure 3. Effect of ionic concentration on the binding of pKID and KID to the KIX on the QCM: a) maximum binding amounts (Δm_{max}), and b) the association constants (K_a). [pKID] = [KID] = (10 mM HEPES, pH 7.9, 5 mM $MgCl_2$, 0.1 mM EDTA, 0.1 % Nonidet P-40, 20 °C).

The K_a values for the nonphosphorylated KID to immobilized KIX also decreased as ionic strength increased (Figure 3b), indicating that the KID–KIX interaction is electrostatic. In contrast, K_a values for the phosphorylated KID do not simply decrease as ionic strength increases. This is in agreement with a previous report, in which a GST (glutathione-S-transferase)–KIX affinity resin was used to perform binding assays.[9] Thus, the pKID phosphate group does not produce a simple electrostatic interaction. NMR spectroscopy showed that the pKID phosphate group of pSer-133 interacts with both Tyr-658 and Lys-662 of the KIX, possibly forming multiple, favorable interactions with these residues, including, possibly, hydrogen bonding.[23] Quantum chemical calculations also suggest that key contributions to stabilization of the complex arise not only from electrostatic interactions, but also from low-barrier hydrogen bonds between pSer-133 and Lys-662.[24]

Kinetic analyses (curve fittings) of peptide binding to QCM: Binding kinetics can be also calculated from the time-dependence of frequency decreases (mass increases) in Figure 2a. Binding between pKID or KID peptides and QCM-immobilized KIX can be determined by Equation (2).

$$\mathrm{KID}+\mathrm{KID}\underset{k_{-1}}{\overset{k_1}{\rightleftharpoons}}\mathrm{KIX/KID} \qquad (2)$$

Binding amounts formed at time t are given by Equations (3)–(5) below.

$$[\mathrm{KIX/KID}]_t = [\mathrm{KIX/KID}]_\infty\{1-\exp(-t/\tau)\} \qquad (3)$$

$$\Delta m_t = \Delta m_\infty\{1-\exp(-t/\tau)\} \qquad (4)$$

$$\tau^{-1} = k_1[\mathrm{KID}] + k_{-1} \qquad (5)$$

Figure 4 shows a linear correlation of the reciprocal of the relaxation time of the binding (τ^{-1}) against various concentrations of the pKID and KID peptides [Eq. (5)].

Association rate constants (k_1) and dissociation rate constants (k_{-1}) were obtained from the slope and intercept, respectively, of Figure 4 and are summarized in Table 1. The association constant (K_a) for pKID ($93\pm2\times10^3$) was approximately 20 times larger than that for KID ($5\pm1\times10^3\,\mathrm{M}^{-1}$), and K_a values obtained from the curve-fitting method [Eq. (5)] were very consistent with those obtained from the saturation method [Eq. (1)]. The 20-fold larger K_a value for pKID compared to KID can be explained by a 20-fold smaller dissociation rate constant (k_{-1}) for pKID compared to KID, as the association rate constants (k_1) for both pKID and KID were essentially identical. Thus, phosphorylation of KID at Ser-133 produces a slow dissociation of pKID from the KIX domain.

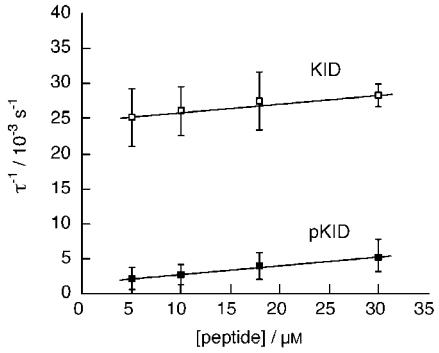

Figure 4. Linear reciprocal plots of the relaxation time (τ) against the concentration of pKID and KID according to Equation (5).

Kinetic analysis also showed that the phosphate group on KID pSer-133 reduces the dissociation rate constant (k_{-1}) by one order of magnitude, resulting in the apparent enhancement of KIX affinity. On the other hand, association rate constants (k_1) were hardly influenced by phosphorylation, indicating that the interaction promoted through this KID phosphoryl group is consistent with hydrogen bonding. Huang et al. reported effects of receptor phosphorylation on the binding kinetics between IRS-1 (insulin receptor substrate-1) and IGF-1R (insulin-like growth factor-1 receptor).[25] Both activated and inactivated IGF-1R display high affinity towards IRS-1, although the activated form binds to IRS-1 with an affinity one order of magnitude greater than the inactivated form, due to a 10-fold larger association rate constant (k_1). In this case, phosphorylation of the several tyrosine residues of IGF-1R considerably changes the electrostatic charges on the surface of the protein, with the result that strong electrostatic interactions from multiple negative charges contribute to the enhanced association rate.

CD spectrum analyses in bulk solution: Binding of KID peptides to KIX was also confirmed from CD spectra changes in bulk aqueous solution. CD spectra confirm that both phosphorylated and nonphosphorylated KIDs exist in random-coil conformations in solution.[9] From NMR spectroscopic analysis, both KID and KIX within the complex were expected to exhibit α-helical conformations.[26] Figure 5a and b show typical CD spectra for these complexes, indicating conformational changes for phosphorylated and nonphosphorylated KIDs in the absence and presence of KIX in buffer solution. When KIDs were added to the KIX solution, the observed molecular ellipticity at 222 nm (θ_{222}) decreased dramatically, due to the formation of α-helical structures within the peptides. The variation in θ_{222} values as a function of KID concentration is shown in Figure 5c; a decrease in the ellipticity at 222 nm is the result of an increase in the α-helical content of KIDs. These results indicate that both phosphorylated and nonphosphorylated KIDs change from random coils to α-helical conformations, due to interactions with KIX. The concentration dependence of these structural changes is consistent with the binding results obtained from QCM analysis.

In conclusion, the binding of KID peptides to the immobilized KIX domain was increased by KID phosphorylation. The increase in association constant (K_a) can be explained by the decrease in dissociation rate constant (k_{-1}) for the pKID compared with that observed for KID to the KIX domain. We believe that the QCM technique will provide a useful tool for obtaining kinetic and quantitative information on protein–protein interactions, enabling the detection

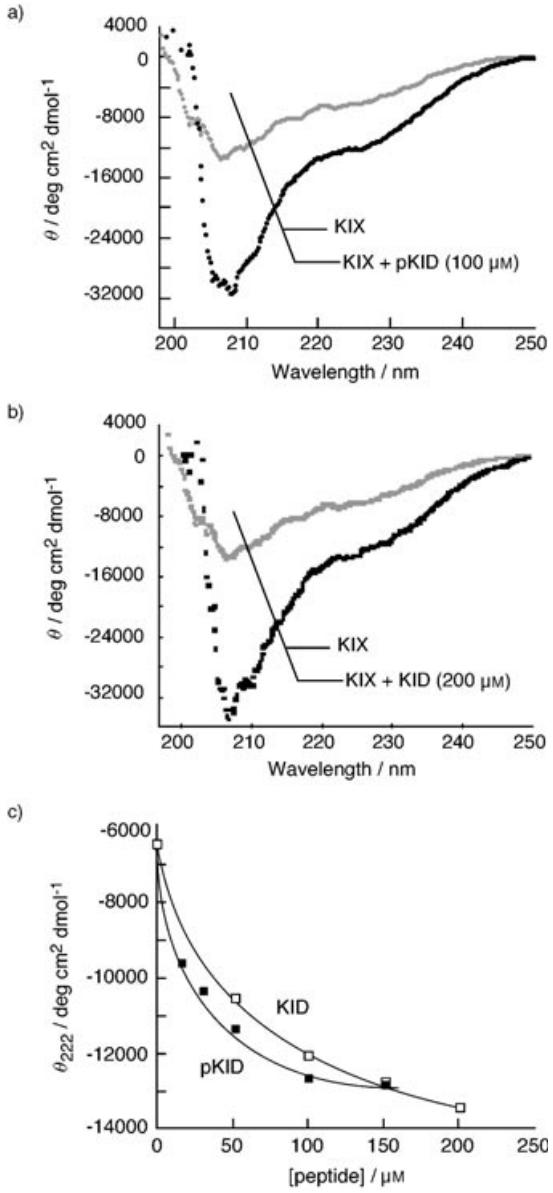

Figure 5. CD spectra changes due to the formation of complexes: a) KIX (5 μM)–pKID (100 μM), b) KIX (5 μM)–KID (200 μM) in 10 mM sodium phosphate, pH 7.4, 20 °C. c) Molar ellipticity changes at 222 nm as a function of the concentration of pKID and KID.

of more complex interactions between protein factors in processes such as gene replication or translation.

Experimental Section

Materials: DNA fragments for the synthesis and PAGE purification of the KIX gene were obtained from Amersham Bioscience (Tokyo, Japan). Fragment A (120-mer): 5′-CCCTCGTAGCAATAGTGTG-GATCCTGCGGTGGTGGTGTTCGAAAAGGCTGGCATGAA-CATGTGACTCAGGACCTACGGAGTCATCTAGTCCA-TAAACTCGTTCAAGCCATCTTCCCAACT-3′, fragment B (120-mer): 5′-ATCCCTGCTATTAGCAGACTCATACATGTCTCCCTC-CACTTTCTTAGCATAGGCAACCAGGTTCTCCATGCGGC-GATCTTTCAGAGCTGCAGGGTCTGGAGTTGGGAAGATGGCTT-GAAC-3′, and fragment C (105-mer): 5′-GAAAGGAGCAGACACG-CAGAATTCTCATTCTTCTAGTTCTTTTTGTATTTTATA-GATTTTCTCTGCTAATAAATGATAGTATTCATCCCTGCTATTAG-CAGACTC-3′.

pGEX-2T and bulk GST purification modules were purchased from Amersham Bioscience (Tokyo, Japan), and *E. coli* BL21(DE3)pLys were purchased from Novagen (Madison, WI). Fmoc-Ile-Alko-PEG-Resin, Fmoc-Ala-OH, Fmoc-Asn(Trt)-OH, Fmoc-Lys(Boc)-OH, Fmoc-Tyr(*t*Bu)-OH, Fmoc-Val-OH, Fmoc-Arg(Mtr)-OH, Fmoc-Ser(*t*Bu)-OH, Fmoc-Ile-OH, Fmoc-Gly-OH, Fmoc-Glu(O*t*Bu)-OH/H_2O, Fmoc-Gln(Trt)-OH, Fmoc-Asp(O*t*Bu)-OH, NMP, piperidine, HOBt, PyBOP, and DIEA were purchased from WATANABE Chemical IND. (Hiroshima, JAPAN). Fmoc-Ser(PO(PBzl)OH)-OH was purchased from Novabiochem (Tokyo, Japan). NHS was from Wako (Osaka, Japan) and EDC [1-ethyl-3-(3-dimethylaminopropyl)carbodiimide] and GMBS (γ-maleimidobutyric acid *N*-hydroxysuccinimide ester) were from DOJINDO (Kumamato, Japan). All other reagents were from Nacali Tesque (Kyoto, Japan) and used without further purification. Poly(ethylene glycol) (PEG) with primary amino groups at the termini (average Mw: 1050) was a gift from NOF (Tokyo, Japan). The molecular weight of the original PEG was calculated following titration of the hydroxyl groups at both ends, and the content of amino groups was calculated from HPLC to be more than 95%.

Preparation of the KIX domain peptide: The KIX domain peptide (residues 586–666 of mCBP plus the GSCGG linker at the N terminus, see Figure 1a) was prepared by expression as a GST–KIX fusion protein, followed by thrombin protease cleavage at the linker region.[27] The inclusion of a Cys residue in the N-terminal linker enabled covalent immobilization of the peptide onto the QCM resonator, by providing a mercapto group linkage mediated by maleimido coupling groups (Figure 1b). A 303-bp fragment including the KIX gene was amplified from the three DNA fragments A, B, and C, which encoded N-terminal, central, and C-terminal regions of the KIX gene, respectively, by using PCR primers Pr-1 (5′-CCCTCGTAGCAATAGTGTGGA-3′) and Pr-2 (5′-GAAAG-GAGCAGACACGCAGAA-3′). After amplification, the reaction mixture was concentrated and digested with *Bam*HI and *Eco*RI to give the 257-bp *Bam*HI–*Eco*RI fragment. The pGEX-2T expression vector was also *Bam*HI- and *Eco*RI-cleaved, treated with alkaline phosphatase, and ligated with the 257-bp fragment. *E. coli* BL21(DE3)pLys cells were transformed with the expression vector and grown at 30 °C in 2×YT media to OD_{600} ~0.6 before induction with 1 mM IPTG (isopropyl-β-D-thiogalactoside). The cells were harvested 5 h after the addition of IPTG. The cell pellet was resuspended in MES buffer (25 mM, pH 6.0) containing glucose (50 mM), NaCl (100 mM), DTT (dithiothreitol, 1 mM), and PMSF (phenylmethylsulfonyl fluoride, 0.1 mM), and the crude lysate was prepared by sonication. Cell debris was centrifuged for 2 h at 9300 g, and the supernatants were collected. Glutathione Sepharose 4B (500 μL) was added to the supernatants and gently mixed by shaking on a rotary shaker at 4 °C for 10 min. After fivefold washing with PBS, thrombin (37.5 U in 1 mL PBS) was added and mixed gently by shaking on a rotary shaker at room temperature for 2 h. (The thrombin recognizes the sequence DLVPR-GS in the peptide and cuts it as indicated by the hyphen.) After centrifugation, the supernatant containing the target peptide was collected and loaded onto a Sephadex G-75 column for purification. The eluted peptide fractions were concentrated with an Ultrafree-4 Centrifugal Filter Unit (MILLIPORE®). SDS-PAGE confirmed that the peptide solution was nearly homogeneous. The identity and integrity of the protein was confirmed by matrix-assisted laser-desorption ionization time-of-flight mass spectrometry (MALDI-TOF MS): *m*/*z*: 9894.24 $[M+H]^+$ (calcd: 9896.73).

Preparation of the KID peptide: The KID peptide (residues 106–151 of mCREBα, see Figure 1a) was prepared by solid-phase peptide synthesis using standard Fmoc-based procedures.[28]

Coupling reactions were performed with Fmoc-Ile-PEG resin (250 mg, 47.5 μmol) and Fmoc amino acid derivative (143 μmol) in the presence of PyBOP [benzotriazole-1-yl-oxy-tris(pyrrolidino)phosphonium, 143 μmol], HOBt (1-hydroxybenzotriazole, 143 μmol), and DIEA (*N,N′*-diisopropylethylamine, 286 μmol) in NMP (*N*-methylpyrrolidone, 2 mL) for 15 min. The coupling reaction was repeated until it was completed, as monitored by the Kaiser test.[28] Removal of Fmoc groups was performed by treatment with 20% piperidine–NMP. These steps were sequentially repeated to polymerize the target peptide, and after final deprotection of the

Fmoc group, the peptides were cleaved from the resin by the following procedure. Resins (100 mg) were dried in vacuo, mixed with a cleavage mixture containing thioanisole (1.34 mL), *m*-cresol (0.2 mL), and TFA (6.65 mL), and stirred at room temperature for 1 h, after which the mixture was filtered. The filtrate (50 mL) was placed in a three-necked, round-bottomed flask equipped with a nitrogen inlet. The flask was cooled in an ice/water bath, *m*-cresol (0.2 mL), 1,2-ethanedithiol (0.3 mL), and trimethylsilyl bromide (0.2 mL) were added, and the reaction mixture was stirred for 1 h. After removal of solvent in vacuo, cooled diethyl ether was added to the residue to precipitate the peptide. The precipitate was washed five times with cooled diethyl ether and the solvent was evaporated to give a crude product. The phosphorylated KID (pKID) peptide, in which the Ser-133 residue was phosphorylated, was synthesized in the same manner, with the exception that the Fmoc-Ser(*t*Bu)-OH derivative was substituted by the Fmoc-Ser(PO(Pbzl)OH)-OH derivative.[29] The crude product was desalted by Sephadex G-10 chromatography in 5% acetic acid. Purification was performed by using reverse-phase HPLC with a Cosmosil 5C18AR-II (Nacarai Tesque, 10× 250 mm) and linear gradient of acetonitrile:water with 0.1% trifluoroacetic acid (25 to 57% acetonitrile in 80 min, flow rate: 2 mL min^{-1}). Each peptide was purified to more than 96%, confirmed by MALDI-TOF MS; KID: *m*/*z*: 5190.16 $[M+H]^+$ (calcd: 5189.35); pKID: m/z: 5269.16 $[M+H]^+$ (calcd: 5268.32).

The 27 MHz QCM system and its calibration: A schematic illustration of a 27 MHz QCM system (AffinixQ, Initium Inc., Tokyo, http://www.initium2000.com) is shown in Figure 1b.[13–18] AT-cut crystals (2.5 mm electrode diameter) were supplied with gold-coated electrodes, formed by thermal evaporation of gold to an average thickness of 100 nm. One side of the quartz crystal was sealed with silicon rubber to maintain it in an environment of air, avoiding contact with the ionic aqueous solution, while the other side was exposed to aqueous buffer solution. A cased 27 MHz QCM was connected to an oscillation circuit, causing the QCM to oscillate at its F_0 close to 27 MHz in aqueous solution.

Sauerbrey's equation was obtained for the AT-cut shear mode QCM[19] [Eq. (6)]:

$$\Delta F = -\frac{2{F_0}^2}{A\sqrt{\rho_q \mu_q}}\Delta m \qquad (6)$$

in which ΔF is the measured frequency change [Hz], F_0 the fundamental frequency of the QCM (27×10^6 Hz), Δm the mass change [g], A the electrode area (4.9 mm^2), ρ_q the density of quartz (2.65 g cm^{-3}), and μ_q the shear modulus of quartz (2.95×10^{11} dyn cm^{-2}). Under ideal conditions,[13–18] a mass increase of 0.62 ng cm^{-2} per 1 Hz of frequency decrease is expected. However, when the QCM is employed in an aqueous solution, Equation (6) cannot be applied, due to effects of interfacial liquid properties (i.e., density, viscosity, elasticity, conductivity, and dielectric constant), thin-film viscoelasticity,[30–32] electrode morphology,[33–36], and the impact of the mechanism of acoustic coupling on the QCM oscillation behavior.[37,38] Therefore, we directly calibrated the relationship between ΔF and Δm by using stepwise immobilization of the KIX peptide by means of a PEG-spacer linkage on the Au electrode of a QCM, similar to the KID–KIX peptide–peptide binding experimental conditions (see below). Thus, both the frequency decrease in the solution (ΔF_{aq}) and the ΔF_{air} after drying in air were measured, in which ΔF_{air} reflects an ideal mass change. There was a good linear correlation between ΔF_{aq} and ΔF_{air}, with the slope calculated to be 2.03 (see Figure S1 of Supporting Information). This indicates that, for these conditions in water, an increase in mass of 0.31 ± 0.02 ng cm^{-2} corresponds to a decrease in frequency of one Hz. The noise level of the 27 MHz QCM was ±2 Hz in buffer solution at 30 °C, and the standard deviation of the frequency was ±2 Hz for 2 h in buffer solution at 30 °C.

Immobilization of the KIX peptide on the QCM Au electrode: Six steps comprising the immobilization scheme of the KIX domain peptide to an Au electrode (4.9 mm^2) of a QCM plate are shown in Figure 1c.[39,40] To prevent any nonspecific interactions on the electrode surface during measurement, PEG molecules known to inhibit nonspecific interactions were used as a spacer to immobilize the KIX peptide.[41] The degree of immobilization at each step was confirmed directly from frequency decreases (mass increases) by using the QCM in water.

Step 1: The bare Au electrode of the QCM resonator was cleaned with piranha solution (one part 30% H_2O_2 in three parts concentrated H_2SO_4) to remove organic contamination from the gold surfaces, followed by rinsing with Milli-Q water several times. (*Caution: Piranha solution should be handled with extreme care, and only small volumes should be prepared at any one time.*)

Step 2: DTDPA (3,3-dithiodipropionic acid, 100 μL of 1 mM aqueous solution) was placed onto the Au electrode and left for 1 h at room temperature, then rinsed with Milli-Q water several times. The frequency decrease before and after immobilization of DTDPA showed that $\Delta m \sim 80\pm23$ ng cm^{-2} (380 ± 109 pmol cm^{-2}) of DTDPA was immobilized on the Au surface, indicating DTAPA coverage to be a monolayer on the electrode surface.

Step 3: For activation of DTAPA carboxylic acids on the Au electrode, 50 μL of a solution—prepared by mixing equivalent volumes of aqueous solutions of NHS (*N*-hydroxysuccinimide, 100 mg mL^{-1}) and EDC (1-ethyl-3-(3-dimethylaminopropyl)carbodiimide, 100 mg mL^{-1})—was placed onto the electrode and left for 20 min at room temperature, then rinsed twice with Milli-Q water.

Step 4: A PEG solution (Mw: 1050, 50 μL of 10 mM in 10 mM of HEPES buffer, pH 8.0) was placed onto the QCM electrode and left for 1 h at room temperature, then rinsed with Milli-Q water several times. From the QCM measurement, 25 ± 2 ng cm^{-2} (24 ± 2 pmol cm^{-2}) of diamino-PEG was immobilized on the Au surface, corresponding to the reaction of one molecule of PEG per 16 molecules of surface-activated DTDPA.

Step 5: A HEPES buffer solution (100 μL of 10 mM, pH 8.0) containing 2 mM GMBS (the *N*-hydroxysuccinimide ester of γ-maleimidobutyric acid) was deposited onto the electrode and incubated for 1 h at room temperature, then rinsed with Milli-Q water several times. A mass decrease ($\Delta m = -3.7\pm2$ ng cm^{-2}) was observed. Ideally, if all free, primary PEG amino groups react with NHS groups, a mass increase of 6.8 ng cm^{-2} is expected. This experimental value was too small to estimate precisely the efficiency of reaction coupling.

Step 6: KIX peptide solution (20 μL in PBS) was deposited onto the QCM electrode and left for 6 h at 4 °C, then rinsed with PBS several times. A mass increase ($\Delta m = 120\pm24$ ng cm^{-2}, i.e., 12.1 ± 2.4 pmol cm^{-2} of KIX) was observed, indicating that one molecule of KIX reacted per two molecules of immobilized PEG. The amount of immobilized KIX peptide did not increase during reaction periods of 6–12 h; therefore, we concluded that the KIX peptide was sufficiently saturated on the electrode after 6 h of reaction.

Reactions at each step were also confirmed by XPS (X-ray photoelectron spectroscopy), performed on an ESCA 850M (SHIMADZU) instrument using an $Mg_{K\alpha}$ X-ray source (1253.6 eV) with pass energy of 100 eV. Usually, the accumulative routine was used for spectral acquisition. Base pressure in the sample chamber was less than 10^{-6} Pa. Spectra were recorded for carbon and nitrogen; the high resolution N_{1s} region of the XPS spectra is displayed in Figure 6. A strong signal at a binding energy of 402.9 eV was observed in the N_{1s} spectrum for the KIX peptide-immobilized surface (after step 6). On the other hand, a weak signal was observed in the spectrum for the PEG-immobilized surface (after step 4) and the GMBS-immobilized surface (after step 5). Normalized intensities of the N_{1s} to the C_{1s} peak areas were found to be 8.5 ± 2.1 for the PEG-immobilized surface, 6.2 ± 1.9 for the GMBS-immobilized surface, and 18 ± 1 for the KIX peptide-immobilized surface. The KIX peptide-modified surface showed the greatest N_{1s} intensity. The original XPS charts of N 1s and C 1s for each immobilization step, and a linear correlation between peak areas of N_{1s}/C_{1s} and atom number ratios of N/C are represented in Figures S2 and S3, respectively, of the Supporting Information.

Binding of the pKID or KID peptides to the KIX-immobilized QCM surface: The KIX domain peptide-immobilized QCM resonator was soaked in an aqueous solution (1.5 mL; 10 mM HEPES buffer, pH 7.9, 0–800 mM NaCl, 5 mM $MgCl_2$, 0.1 mM EDTA, and 0.1% Nonidet P-40) and the resonance frequency of the QCM was defined as zero position after equilibrium (ca. 10–20 min). The frequency decrease of the QCM resonator, responding to the addition of KID peptide solutions of varying solution conditions (concentration and ionic strength), was then recorded over time. The solution was stirred to avoid any effect of diffusion of peptides, and the stirring did not affect the stability and the extent of QCM frequency changes. Measurements were performed over a range of 5–25 °C.

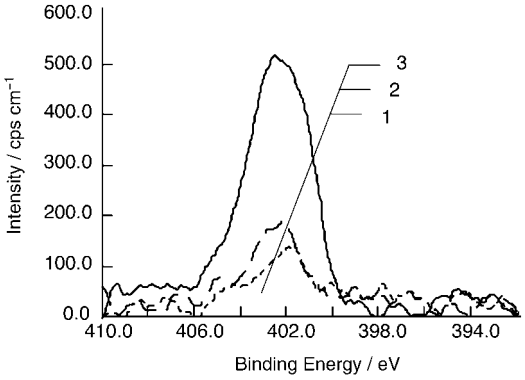

Figure 6. XPS spectra at the N_{1s} region of three samples, on which 1) PEG, 2) GMBS, and 3) KIX were immobilized.

CD spectroscopic analysis: CD spectra were observed using a J-720WI spectropolarimeter (JASCO) using a quartz cell (2 mm cell length, 10 mM sodium phosphate, pH 7.4). Initially, the CD spectrum of only KIX was observed. Following incubation with KID for 30 min the spectrum of KID–KIX was observed at 20 °C in aqueous media (no QCM). The concentration of peptides was determined from the absorbance at 280 nm, using an extinction coefficient of 1.28 mM^{-1}cm^{-1} for pKID.[11]

Acknowledgement

We thank NOF Co. (Japan) for the generous gift of diamino-PEG. H.M. gives thanks to Research Fellowships of the Japan Society for Promotion of Science for Young Scientists. This work was partly supported by a Grant-in-Aid for Science Research from the Ministry of Education, Science, and Culture Japan, and CREST, Japan Science and Technology Corporation.

[1] M. Karin, T. Hunter, *Curr. Biol.* **1995**, *5*, 747–757.
[2] G. Orphanides, T. Lagrange, D. Reinberg, *Genes Dev.* **1996**, *10*, 2657–2683.
[3] T. Hunter, M. Karin, *Cell* **1992**, *70*, 375–387.
[4] M. R. Montminy, L. M. Bilezikjian, *Nature* **1987**, *328*, 175–178.
[5] A. J. Shaywitz, M. E. Greenberg, *Annu. Rev. Biochem.* **1999**, *68*, 821–861.
[6] P. K. Brindle, M. R. Montminy, *Curr. Opin. Genet. Dev.* **1992**, *2*, 199–204.
[7] J. C. Chrivia, R. P. Kwok, N. Lamb, M. Hagiwara, M. R. Montminy, R. H. Goodman, *Nature* **1993**, *365*, 855–859.
[8] R. P. Kwok, J. R. Lundblad, J. C. Chrivia, J. P. Richards, H. P. Bachinger, R. G. Brennan, S. G. Roberts, M. R. Green, R. H. Goodman, *Nature* **1994**, *370*, 223–226.
[9] D. Parker, K. Ferreri, T. Nakajima, V. J. Lamorte, R. Evans, S. C. Koerber, C. Hoeger, M. R. Montminy, *Mol. Cell. Biol.* **1996**, *16*, 694–703.
[10] D. Parker, M. Rivera, T. Zor, A. Henrion-Caude, I. Radhakrishnan, A. Kumar, L. H. Shapiro, P. E. Wright, M. R. Montminy, P. K. Brindle, *Mol. Cell. Biol.* **1999**, *19*, 5601–5607.
[11] I. Radhakrishan, G. C. Perez-Alvarado, D. Parker, H. J. Dyson, M. R. Montminy, P. E. Wright, *Cell* **1997**, *91*, 741–752.
[12] A. J. Shaywitz, S. L. Dove, J. M. Kornhauser, A. Hochschild, M. E. Greenberg, *Mol. Cell. Biol.* **2000**, *20*, 9409–9422.
[13] Y. Okahata, M. Kawase, K. Niikura, F. Ohtake, H. Furusawa, Y. Ebara, *Anal. Chem.* **1998**, *70*, 1288–1296.
[14] Y. Okahata, K. Niikura, Y. Sugiura, M. Sawada, T . Morii, *Biochemistry* **1998**, *37*, 5666–5672.
[15] H. Furusawa, Y. Kitamura, N. Hagiwara, T. Tsurimoto, Y. Okahata, *ChemPhysChem* **2002**, *3*, 446–448.
[16] K. Niikura, H. Matsuno, Y. Okahata, *J. Am. Chem. Soc.* **1998**, *120*, 8537–8538.
[17] H. Matsuno, K. Niikura, Y. Okahata, *Chem. Eur. J.* **2001**, *7*, 3305–3312.
[18] H. Matsuno, H. Furusawa, Y. Okahata, *Chem. Commun.* **2002**, 470–471.
[19] G. Sauerbrey, *Z. Phys.* **1959**, *155*, 206–222.
[20] A. Janshoff, H. J. Galla, C. Steinem, *Angew. Chem.* **2000**, *112*, 4164–4195; *Angew. Chem. Int. Ed.* **2000**, *39*, 4004–4032.
[21] Y. Ebara, K. Itakura, Y. Okahata, *Langmuir*, **1996**, *12*, 5165–5170.
[22] K. Denbigh, *The Principles of Chemical Equilibrium*, Cambridge University Press, New York, **1995**.
[23] A. P. Mestas, K. J. Lumb, *Nat. Struct. Biol.* **1999**, *6*, 613–614.
[24] M. D. Peraro, F. Alber, P. Carloni, *Eur. Biophys. J.* **2001**, *30*, 75–81.
[25] M. Huang, W. P. Lai, M. S. Wong, M. Yang, *FEBS Lett.* **2001**, *505*, 31–36.
[26] I. Radhakrishan, G. C. Perez-Alvarado, H. J. Dyson, P. E. Wright, *FEBS Lett.* **1998**, *430*, 317–322.
[27] D. B. Smith, K. S. Johnson, *Gene* **1988**, *67*, 31–40.
[28] G. B. Fields, R. L. Nobel, *Int. J. Peptide Protein Res.* **1990**, *35*, 161–214.
[29] T. Wakamiya, R. Togashi, T. Nishida, K. Saruta, J. Yasuoka, S. Kusumoto, S. Aimoto, K. Yoshizawa-Kumagaya, K. Nakajima, K. Nagata, *Bioorg. Med. Chem.* **1997**, *5*, 135–145.
[30] T. Nomura, M. Okuhara, *Anal. Chim. Acta* **1982**, *142*, 281–283.
[31] S. Bruckenstein, M. Shay, *Electrochim. Acta* **1985**, *30*, 1295–1298.
[32] K. K. Kanazawa, J. Gordon, *Anal. Chim. Acta* **1985**, *175*, 99–103.
[33] M. Yang, M. Thompson, W. C. Duncan-Hewitt, *Langmuir* **1993**, *9*, 802–806.
[34] W. Hinsberg, C. Wilson, K. K. Kanazawa, *J. Electrochem. Soc.* **1986**, *133*, 1448–1451.
[35] Y. Okahata, H. Ebato, *Anal. Chem.* **1989**, *61*, 2185–2188.
[36] Y. Okahata, K. Kimura, K. Ariga, *J. Am. Chem. Soc.* **1989**, *111*, 9190–9192.
[37] M. Yang, M. Thompson, *Langmuir* **1993**, *9*, 1990–1993.
[38] M. Urbakh, L. Daikhin, *Langmuir* **1994**, *10*, 2836–2839.
[39] S. Fukusho, H. Furusawa, Y. Okahata, *Chem. Commun.* **2002**, 88–89.
[40] H. Furusawa, A. Watanabe, Y. Okahata, unpublished results.
[41] O. Birkert, H. M. Haake, A. Schutz, J. Mack, A. Brecht, G. Jung, G. Gauglitz, *Anal. Biochem.* **2000**, *282*, 200–208.

Received: January 13, 2004
Revised: July 16, 2004
Published online: October 29, 2004